Structures 5 (2016) 141–151

Contents lists available at ScienceDirect

Structures

journal homepage: http://www.elsevier.com/locate/structures

Behavior of GFRP bridge deck panels infilled with polyurethane foam under various environmental exposure

Hesham Tuwair [a], Jeffery Volz [b], Mohamed ElGawady [a,*], Mohaned Mohamed [c], K. Chandrashekhara [c], Victor Birman [d]

[a] Department of Civil, Architectural, and Environmental Engineering, Missouri University of Science and Technology, Rolla, MO, USA
[b] School of Civil Engineering and Environmental Science, The University of Oklahoma, Norman, OK, USA
[c] Department of Mechanical and Aerospace Engineering, Missouri University of Science and Technology, Rolla, MO, USA
[d] Engineering Education Center, Missouri University of Science and Technology, Rolla, MO, USA

ARTICLE INFO

Article history:
Received 28 May 2015
Received in revised form 19 September 2015
Accepted 12 October 2015
Available online 23 October 2015

Keywords:
FRP bridge deck
Durability
Environmental degradation
Sandwich panel
GFRP
Polyurethane foam
Polyurethane resin

ABSTRACT

This paper investigates the performance of polyurethane foam-infill bridge deck panels (PU sandwich panels) after being exposed to various environmental conditions. These panels were constructed with woven E-glass fiber/polyurethane facesheets that were separated by a trapezoidal-shaped, low-density polyurethane foam. Corrugated web layers were introduced into the core to enhance the panel's structural characteristics. The PU panels were manufactured through a one-step vacuum assisted resin transfer molding (VARTM) process. An experimental program was designed to simulate their in situ environments. The environmental conditions used included different conditioning regimens to examine the behavior of both GFRP laminates and PU sandwich panels. The GFRP laminates, which were made from the same materials as the PU sandwich panels, were exposed to ultraviolet radiation, a deicing solution at both room temperature and elevated temperature, and thermal cycling. The PU sandwich panels were exposed to thermal cycling (a series of freeze–thaw, mid–high temperatures, and mid–high relative humidity cycles). The thermal cycling exposure was conducted in a computer-controlled environmental chamber to duplicate seasonal effects in Midwestern states. Following the exposure regimens, tensile strength tests and four-point loading tests were performed on the GFRP laminates and the PU sandwich panels, respectively. The evaluation was based on visual inspection, strength, stiffness, and failure modes, as compared to those that were not conditioned (the control). The results of this study revealed that degradation did exist due to the effects of thermal cycling and the deicing solution. The ultraviolet radiation, however, did not cause any degradation. These results were within the recommended environmental durability design factors of the FHWA guidelines.

1. Introduction

With the continuous deterioration of the nation's infrastructure, it was found that over half of the nation's 607,000 bridges were built before 1940 [1]. These bridges have reached the end of their useful service lives. In a study recently conducted by Ellis [2] for the Federal Highway Administration (FHWA), the estimated annual direct cost of repairing corrosion on highway bridges was between $6.43 and $10.15 billion. This estimate includes the $1.07 to $2.93 billion needed each year to maintain the concrete bridge decks. In an effort to address these sobering statistics, transportation agencies have been trying to identify new, cost-effective, and reliable construction materials that can be used to not only fabricate but also rehabilitate bridge decks. Advanced composites made of fibers embedded in a polymeric resin, also known as fiber-reinforced polymer (FRP) materials, have received considerable attention as a strong candidate to replace deteriorating concrete and steel structures. These composites, commonly used for civil engineering applications, are reinforced with an inexpensive fiberglass. The advantages of FRP composites have been widely recognized and include their low weight, ease of installation (reducing traffic delay), resistance to both environmental and chemical attacks, and resistance to fatigue loads.

Extensive durability studies have been conducted on FRP composites for aerospace and marine applications. Autoclave-based fabrication was used to manufacture each of these applications under strict specifications. Cheaper manufacturing processes have been used in the civil market (e.g., wet layup, vacuum assisted resin transfer molding [VARTM], and pultrusion), resulting in lower temperature cure epoxies. The FRP composites used in the field for rehabilitation purposes are cured under ambient temperatures. Thus, these composites are more vulnerable to moisture damage and plasticization than those used for

* Corresponding author.
E-mail addresses: hrthw2@mst.edu (H. Tuwair), volz@ou.edu (J. Volz), elgawadym@mst.edu (M. ElGawady), mmm7vc@mst.edu (M. Mohamed), chandra@mst.edu (K. Chandrashekhara), vbirman@mst.edu (V. Birman).

http://dx.doi.org/10.1016/j.istruc.2015.10.008
2352-0124/

Fig. 1. Four prototype mid-scale panels.

aerospace and marine applications. Accordingly, it is impossible to interpret the results of those studies established by the Department of Defense for civil engineering applications [3].

Since FRP composites are made through the combination of micron-sized fibers and polymer matrices, the polymer matrix of the FRP composite is considered the weak link as it may experience a change in its physical properties and chemical degradation during environmental exposure. Polymer composites are vulnerable to ultraviolet radiation, both freeze–thaw and high temperature cycles, moisture, deicing chemicals, and alkali attacks, leading to degradation in strength and stiffness [4–16].

A number of studies have been conducted on the effects on the durability of FRP composites. Among those, Karbhari and Pope [14] and GangaRao et al. [15] investigated the impact of freeze–thaw cycles on these composites. They found that such exposure can negatively change the thermo-mechanical response of the resin. Another study, conducted by Verghese et al. [17], found that degradation is primarily associated with the micro-cracking that occurs when the volume of absorbed water changes. Jamond et al. [18] and Malvar et al. [19]) investigated several commercial composites under environmental exposure. They found that seawater immersion and salt-fog exposure caused the greatest degradation in mechanical properties. Lopez-Anido et al. [16] investigated the performance of the adhesive bonds of the FRP composite under freeze–thaw cycles. They noted that the bond was reduced significantly and the failure mode was changed. Connolly et al. [20] reported changes in the physical properties of the following: the pultruded polyurethane, the vinyl ester, the unsaturated polyester, and the unsaturated polyester–urethane hybrid composites under ultraviolet radiation, salt water, hydrocarbon fluids, and strong acid solutions. They found that the polyurethane pultruded composites exhibited superior strength and toughness under environmental exposure, when compared to the other examined composites.

Polyurethane resin has better properties than traditional resin systems (e.g., polyester and vinyl ester resin systems) [20]. Additionally, the polyurethane composites' profiles have exhibited promising preliminary results in environmental exposure tests. Glass-fiber-reinforced polyurethane composites are conventionally manufactured using a pultrusion process. However, pultrusion is limited to the manufacture of constant cross-section profile composite parts. The VARTM process is a low-cost composite manufacturing process that is widely used throughout the composite industry. This process has been developed over the last two decades for applications in commercial, military, and marine composite structures [21]. However, viscosity and pot-life limitations of polyurethane resins have prevented its use with the VARTM process until recently when a major development in novel catalysis chemistry was developed by Bayer MaterialScience. This dual catalyst system extended the pot life of mixed resins at room temperature [22]. The resin itself was developed quite recently. Thus, the durability studies of glass-fiber-reinforced polyurethane composites, manufactured with low cost VARTM process under harsh environmental conditions for infrastructure applications, has not been reported in the literature.

This study presents an experimental work that investigates the effects of environmental exposure on the behavior of both GFRP laminates and PU sandwich panels containing a new-generation two-part thermoset polyurethane resin from Bayer MaterialScience. The panel was previously proposed by Tuwair et al. [23]. The prototype PU sandwich panels were comprised of two woven E-glass fibers/polyurethane facesheets that were separated by a trapezoidal-shaped, low-density, polyurethane foam (see Fig. 1). The foam core was comprised of stiff web layers that served as a truss structure between the facesheets. The VARTM process was used to manufacture these PU sandwich panels.

2. Experimental program

Testing the entire sandwich panel under different environmental conditions is essential to determine the full stiffness and strength degradation and mode of failure of the panel. However, this type of test cannot provide the degradation data for each constituent material of the PU sandwich panels. Thus, testing was conducted on small coupon specimens of the GFRP material in addition to PU sandwich panels. The conditioning regimens conducted in this study consisted of exposure to ultraviolet radiation, a deicing solution at both room temperature and an elevated temperature, and thermal cycling (a series of freeze–thaw, mid–high temperatures, and mid–high relative humidity cycles). Each test was conducted in a computer-controlled environmental chamber.

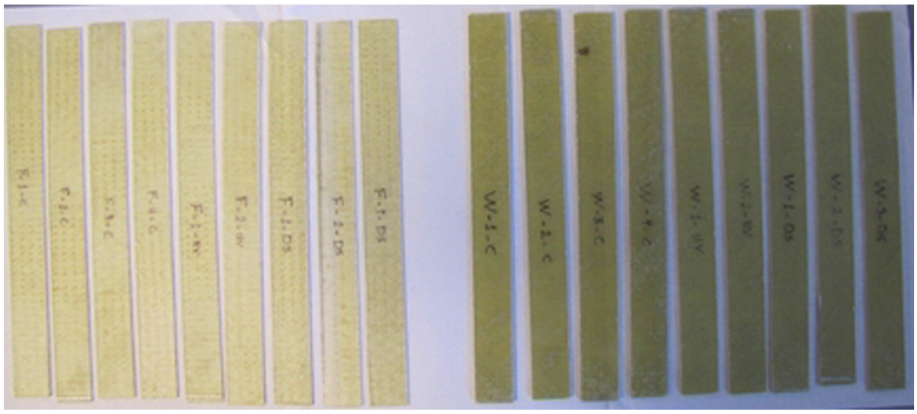

Fig. 2. Coupon specimens of GFRP laminates.

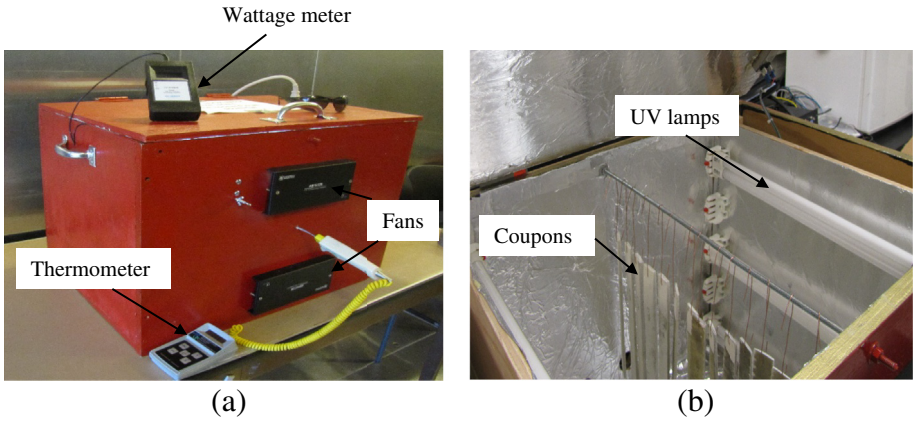

Fig. 3. UV chamber: (a) outside view and (b) inside view.

2.1. GFRP laminate characterization

The GFRP laminates examined in this study were manufactured in the Composite Manufacturing Laboratory of the Mechanical and Aerospace Engineering Department at Missouri University of Science and Technology. These laminates were made to represent the facesheet and web core of the PU sandwich panels. The facesheet laminate was comprised of three plies of plain-weave woven E-glass fabric (WR18/20) laid up equally in a 0/90° fiber orientation. The web core laminate was formed from three plies of ±45° laid up equally in a double bias of E-glass woven fabric (E-BXM1715). Coupon specimens were taken out of facesheets and webs without disturbing the fiber angles (i.e., with fiber 0/90° for the coupons out of the facesheets and ±45° for those out of the webs). Each of the facesheet and web core laminates contained 9.73 oz./sq.yd. (330 g/m^2) and 8.96 oz./sq.yd. (304 g/m^2) of E-glass fibers in their longitudinal and transverse directions, respectively. The matrix material used for the specimens consisted of a new-generation two-part, thermoset polyurethane resin. The "A" component of the resin was an Isocyanate NB#840,859 ISO, Diphenylmethane Diisocyanate (MDI-Aromatic), while the "B" component was a low viscosity (350 cP) Polyol (RTM NB#840,871). The components react rapidly after mixing to form a highly cross-linked thermoset polymer with excellent thermal stability and mechanical properties. It features a longer pot life which enabled it to be used with the VARTM process.

The facesheet and web core laminates were cut into 50 coupon specimens (see Fig. 2) so that their in-plane tensile properties, before and after the environmental conditioning, could be examined. ASTM D3039/D3039M standard [24] recommends that the minimum length of the specimen be taken as the gripping length at both ends, plus two times the coupon width, plus a gage length. The width should also be taken as needed. As such, the coupon dimensions were 10 in. (254.00 mm) long and 1 in. (25.4 mm) wide. Aluminum end tabs of a length of 2.5 in. (63.50 mm) were placed one day before the testing. Between four and five coupon specimens were typically considered for the control specimens and for every conditioning regimen specimens.

An MTS880 universal testing machine with wedge-type mechanical grips was used to conduct tensile strength tests on the control and the conditioned specimens. The speed of the test was set to provide a constant strain rate within a gage length of 0.01 min^{-1}, as recommended by the standard, which is 0.05 in/min (1.27 mm/min). One electric resistance strain gauge with a length of 0.236 in. (6.00 mm) and a resistance of 350 ± 0.2 Ω was used to measure the longitudinal strains. A data acquisition system (DAS) was used to record the test data, including load and stroke of the MTS machine.

The mechanical properties of GFRP coupons, namely, the young's modulus and the tensile strength, were used to assess the stiffness and strength. The modulus of elasticity was taken as the highest slope of a straight line from the initial portion of the stress–strain curve. The tensile strength of the material was calculated by dividing the maximum applied load by the initial undeformed cross-sectional area of the coupon.

2.2. Conditioning regimens

2.2.1. Ultraviolet radiation

Glass fiber-reinforced polymer (GFRP) composites are used for long periods of time in outdoor applications (e.g., bridges). As such, these composites are exposed to large amounts of ultraviolet (UV) radiation, which can have a degrading effect. In general, the influence of UV radiation on total solar global radiation is 5–6% (depending on both the location and the time). The UV spectral range observed on Earth's surface

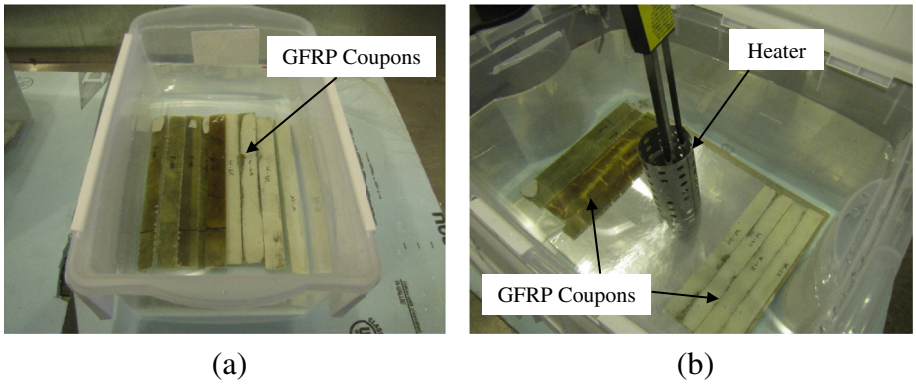

Fig. 4. Deicing exposure: (a) coupon specimens at room temperature and (b) at elevated temperature.

Fig. 5. Environmental test chamber.

varies from approximately 295 to 400 nm [3]. This UV light can alter the molecular chain of polymers, creating microcracks that deteriorate the GFRP's durability.

A UV chamber constructed specifically for this study was used to perform this test. This chamber was made to meet the requirements defined in ASTM G151 [25] and ASTM G154 [26]. Not all of the requirements were strictly followed. The chamber (depicted in Fig. 3) was built from a wooden box and had the following dimensions: 27.5 in. (698.50 mm) long, 19.5 in. (495.30 mm) wide, and 20 in. (508.00 mm) high. These dimensions were used to accommodate the coupon specimens. The desired wattage intensity recommended by the standard was used to determine the box's length. The standard suggested the intensity should be 0.89 W/(m^2·nm) at the specimen's surface. The actual wattage intensity recorded at the specimen's surface, however, was between 0.77 and 0.95 W/(m^2·nm). A wattage meter (Fig. 3a) was used to check the wattage's uniformity. Aluminum foil was used to cover the interior surface of the chamber so that the UV light would be reflected onto the specimens. The ASTM G154 standard [26] suggested that a spectral UV distribution of a UVA 340 lamp be used. A spectral UVA 365 lamp was employed in this study due to its market availability. These lamps were purchased from Worldwide Specialty Lamp (located in Austell, Georgia). Only three UV lamps (see Fig. 3b), placed on each side of the chamber, could provide a reasonable, uniform UV spectrum. These lamps generated a temperature of approximately 167°F (75 °C). Therefore, 8 fans (2 on the top and 2 on the bottom of each longitudinal side), each with a diameter of 1.5 in. (38.10 mm), were created to reduce the temperature to 125°F (51.6 °C) (see Fig. 3a). A light timer was used to cycle the UV light so that each cycle consisted of four hours of UV exposure and four hours of condensation (dark period).

A total of 10 coupon specimens (5 representing the facesheets and 5 for the diagonal web core) were used for the aging regimen. The coupons were hung in the middle of the chamber (as illustrated in Fig. 3b) so that they were equally exposed to the UV light from both sides. An ultraviolet test was conducted in accordance with the ASTM G154 standard [26] to simulate the solar radiation effect created by sunlight. The

Table 1
Thermal cycling regimen.

Cycles	Freeze–thaw	Temperature	Relative humidity (60–95%)		
Temperature range, °F (°C)	−4 (−20) to 50 (10)	68 (20) to 122 (50)	68 (20)	77 (25)	104 (40)
Number of cycles	50	150	50	50	50
Total number of cycles	350				

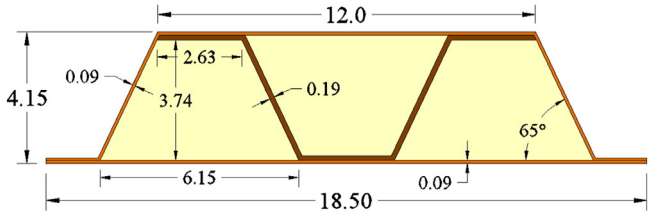

Fig. 6. Schematic of mid-scale panel cross section (all dimensions in inches, 1 in. = 25.4 mm).

testing cycles were in accordance with the ASTM D2508 standard [27]. Each coupon was run through a tension test in accordance with the ASTM D3039/D3039 standard [24] after the predetermined conditioning time was reached. The results were then compared to those taken from the control specimens to evaluate whether or not exposure to the UV environment would reduce the effectiveness of the conditioned specimens.

2.2.2. Deicing solution

Deicing salts are used on bridges during the winter months to reduce traffic accidents, injuries, and fatalities. The deicing chemicals may have adverse effects on the fibers (e.g., a degradation of stiffness and strength). Therefore, the influence of sodium chloride (NaCl) on the behavior of GFRP/PU materials was investigated. This investigation was conducted on two solutions. One tank contained a solution that was maintained at room temperature, and another one contained a solution that was kept at 122°F (50 °C) to accelerate the absorption (see Figs. 4a and 4b). This temperature was below the glass transition temperature (Tg) of the polyurethane resin to prevent any degradation mechanism that might occur at that point. Each tank accommodated 8 coupon specimens (4 for the facesheet and 4 for the diagonal web core) that were immersed in a sodium chloride solution. The deicer solution was comprised of 3% by weight sodium chloride. Conditioning was maintained for 90 days. The coupons were then subjected to tensile tests. These results were compared to those taken from the control specimens to evaluate whether or not the deicing solution reduced the effectiveness of the conditioned specimens.

2.2.3. Thermal cycling

The thermal cycling conditioning, in terms of a series of freeze–thaw, mid–high temperatures, and mid–high relative humidity cycles, was designed to simulate in situ environments. The ASTM C666 standard [28] was followed for the conditioning cycling test. This standard was originally designed for testing the durability of concrete; it was used here as a guide for measuring the durability of composite structures. The computer-controlled environmental chamber used in this study (Model WR-1750) was manufactured by B-M-A, Inc. It is pictured in Fig. 5. It had a temperature range of between 180 °F (82.2 °C) and

Fig. 7. VARTM manufacturing process for mid-scale panels.

Fig. 8. PU sandwich panels within environmental test chamber.

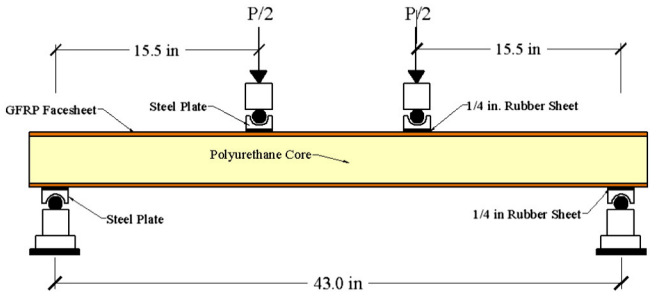

Fig. 10. Schematic of four-point bending flexural test setup (all dimensions in inches, 1 in. = 25.4 mm).

−30 °F (−34.4 °C) and an extensive range of cycling capabilities. The environmental cycle regimen that was used to cycle both temperature and humidity is illustrated in Table 1. This regimen was based on weather data accumulated in the Midwest over the previous 30 years [29].

The conditioning procedure was comprised of three main phases (see Table 1):

1. 50-cycle freeze–thaw phase
2. 50-cycle mid–high temperature phase
3. 150-cycle mid–high relative humidity phase

These phases were used to simulate the effects of the winter and summer seasons. The minimum temperature reached in the freeze–thaw cycles was −4°F (−20 °C), while the maximum temperature reached in the high temperature cycles was 122°F (50 °C). The maximum relative humidity was 95%. Approximately 5 cycles per day were accomplished with 30 min of ramp time and 2 h of hold time for each temperature ring, totaling 73 days required to complete the test exposure. Once all of the phases had been run, the specimens were evaluated based on visual inspection, flexural stiffness, strength, and failure modes, compared to the unconditioned specimens.

2.3. PU sandwich panel characterization

The PU sandwich panels investigated in this study were also manufactured in the Composite Manufacturing Laboratory of the Mechanical and Aerospace Engineering Department at Missouri University of Science and Technology. A schematic of the PU mid-scale sandwich panel cross section is given in Fig. 6. Both the top and the bottom facesheets were constructed with three plies of 0°/90° biaxial E-glass plain weave, woven fabric (WR18/3010); they were manufactured by Owens Corning. The diagonal webs, manufactured by VectorPly, consisted of three plies of +45°/−45° double-bias E-glass, stitch-bonded fabric (EBXM1715) that was integrated with the facesheets. The foam was matted with two plies of +45°/−45° E-glass, knitted fabric to enhance bonding between the foam core and the plies.

The VARTM process was used to manufacture the PU sandwich panels. The mid-scale panels used a two-part thermoset polyurethane resin system that was manufactured by Bayer MaterialScience. A photograph of one of the panels undergoing the VARTM manufacturing process is given in Fig. 7. The specimens were post-cured for 1 h at 160 °F (71.1 °C) and for 4 h at 180 °F (82.2 °C) in a walk-in oven. A total of four mid-scale panels were manufactured with the cross-section (see Fig. 6). Each had an overall length of 47 in. (1193.80 mm). Two of the panels were subjected to a predetermined sequence of thermal cycling conditioning, while the remaining panels were designated as the control panels. A photograph of the four mid-scale PU sandwich panels is given in Fig. 1.

2.3.1. Test procedure

The PU sandwich panels were subjected to the environmental thermal cycling regimen stated in Section 2.2.3. Prior to the thermal exposure in the environmental chamber, the specimens were prepared by protecting their ends with supplemental epoxy coating and waterproof tape (see Fig. 8). This step was necessary because the actual bridge deck panels would completely encapsulate the foam core. The actual weight and dimensions of the specimens were taken before the environmental exposure was begun. The panels were elevated within the environmental chamber to allow air circulation on all sides (see Fig.8). The panels were removed, thoroughly inspected for signs of damage, instrumented with strain gauges, and then placed into the static loading test setup after the required number of days within the chamber was accomplished. The examination included a comparison between the flexural strength, stiffness, and failure mode of the conditioned specimens and the control specimens.

2.3.2. Four-point bending flexural test

Characterization of the durability behavior of the PU sandwich panels was accomplished by testing the PU sandwich panels under the four-point bending tests. A picture of the test-setup is illustrated in Figs. 9 and 10. This test was performed according to the ASTM C393

Fig. 9. Four-point bending flexural test setup.

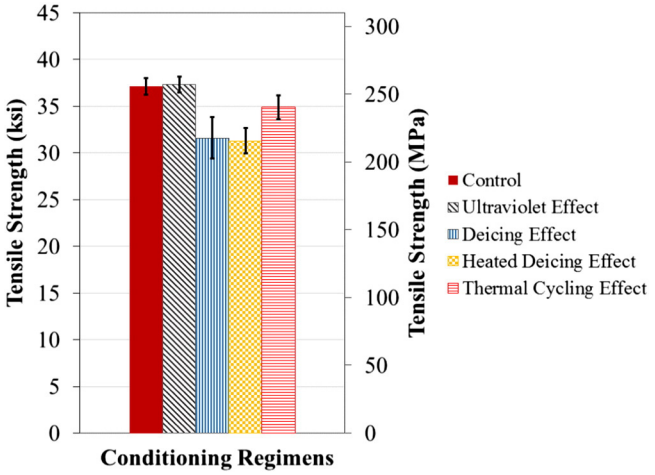

Fig. 11. Tensile strength of facesheet coupons under different regimens.

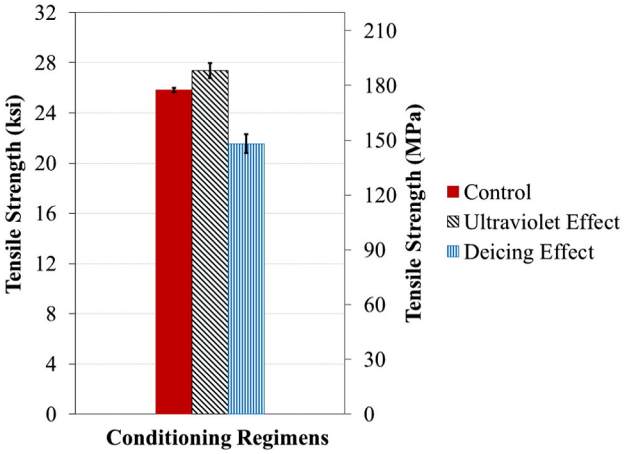

Fig. 13. Tensile strength of web coupons under different regimens.

standard [30]. The objective of this test was to determine the flexural stiffness and strength of the panels. Each panel was tested in one-way bending with a span of 43 in. (1092.20 mm), under two equal point loads applied at 15.5 in. (393.70 mm) from each support, as depicted in Fig. 10. An MTS880 testing machine was used to load the specimen up to failure at a load rate of 0.05 in/min (1.27 mm/min).

Four strain gauges monitored the strain; two were attached in each compression and tension area at the specimen's mid-span. Eight direct current variable transformers (DCVTs) (two at the mid-span, two at each loading point, and one at each end) were used to monitor the displacement at five locations.

3. Experimental results

3.1. Tensile testing results

Figs. 11 and 12 compare the average ultimate tensile strength and tensile modulus of elasticity between the control facesheet specimens and the coupon specimens subjected to ultraviolet radiation, deicing solution at both room temperature and elevated temperature, and thermal cycling. Figs. 13 and 14 compare the average ultimate tensile strength and tensile modulus of the specimens taken from web layers. The black bar shown in each figure represents the standard deviation of the results. These variations in results can be attributed to the quality of laminate manufacture (e.g., percentage of voids and resin-rich areas). A summary of the results is presented in Tables 2–5.

The average results of tensile strength of the control facesheet and web layer coupons were 37.1 ksi (255.8 MPa) and 25.8 ksi (177.9 MPa), respectively, as illustrated in Figs. 11 and 13. The tensile modulus of elasticity of the control facesheet and web layer coupons was 2030 ksi (14.0 GPa) and 1691 ksi (11.7 GPa), respectively (Figs. 12 and 14). All of the facesheet and web core coupons ruptured suddenly in the fiber direction (0° for the facesheet and 45° for the web core) (see Fig. 15). The failure pattern was consistent for all GFRP coupon specimens both with and without environmental conditioning.

A set of coupon specimens was tested under tensile strength after they it was conditioned in ultraviolet radiation for 2000 h. The results gathered from this test are illustrated in Figs. 11–14. A visual inspection revealed that a surface gloss loss and a yellowing of the coupon specimens had occurred (see Fig. 16). Polymers that contain styrene cross-links are particularly prone to the yellowing phenomena. The average weight of the conditioned facesheet and the web layer coupon specimens was reduced by 0.86% and 0.63%, respectively. The fibers, however, were not visible. Cooling fans and thermo-couplers were used to closely control the temperature at 125°F (51.6 °C), which is low enough to not break the bonds in the cured resin. Thus, the weight loss should not be due to heating effects but due to the UV irradiation. The average results of the facesheet coupons indicated that the tensile strength was 37.3 ksi (257.2 MPa), and the tensile modulus of elasticity was 2261 ksi (15.6 GPa) (Figs. 11 and 12). The average results of the web core coupons showed that the tensile strength and tensile modulus of elasticity

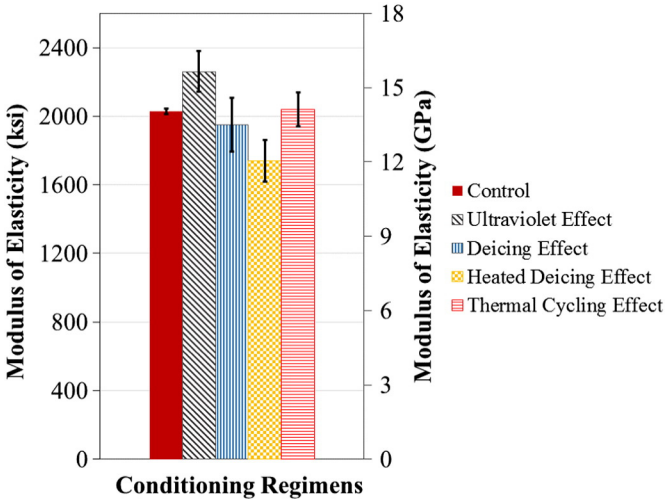

Fig. 12. Tensile modulus of elasticity of facesheet coupons under different regimens.

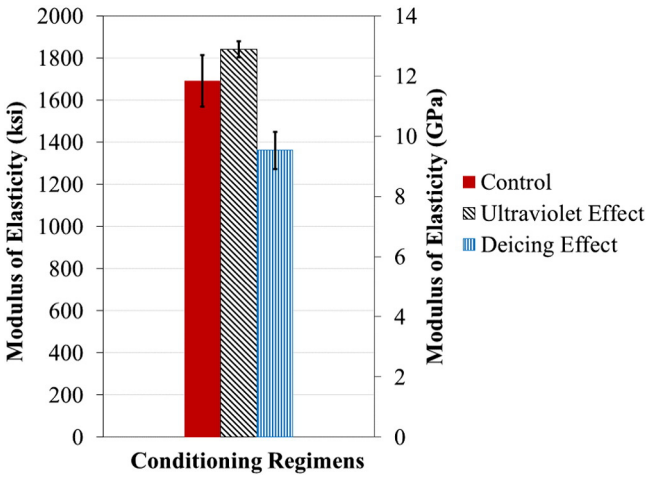

Fig. 14. Tensile modulus of elasticity of web coupons under different regimens.

Table 2
Summary of facesheet coupons' tensile strength results.

Tensile strength	Control	Ultraviolet effect	De-icing effect	Heated deicing effect	Thermal cycling effect
Mean, ksi (MPa)	37.1 (255.8)	37.3 (257.2)	31.6 (217.9)	31.3 (215.8)	34.9 (240.6)
SD, ksi (MPa)	0.89 (6.1)	0.84 (5.8)	2.21 (15.2)	1.32 (9.1)	1.28 (8.8)
CV (%)	2.41	2.25	7.14	4.23	3.68

SD: standard deviation; CV: coefficient of variation.

Table 3
Summary of facesheet coupons' modulus of elasticity results.

Modulus of elasticity	Control	Ultraviolet effect	De-icing effect	Heated deicing effect	Thermal cycling effect
Mean, ksi (GPa)	2030 (14.0)	2261 (15.6)	1949.6 (13.4)	1738.6 (11.9)	2040 (14.0)
SD, ksi (GPa)	15.63 (0.11)	120.30 (0.83)	158.50 (1.09)	120.48 (0.83)	97.51 (0.67)
C.V (%)	0.77	5.32	8.13	6.93	4.78

were 27.4 ksi (188.9 MPa) and 1839.8 ksi (12.7 GPa), respectively, as illustrated in Figs. 13 and 14. The residual tensile strength and residual tensile modulus of elasticity, when compared to the results collected from the control facesheet coupon specimens, were approximately 100.5% and 111.4%, respectively. The residual tensile strength and residual tensile modulus of elasticity of the web core coupons were approximately 106.2% and 108.8%, respectively. Even though the variation of the standard deviation of the conditioned specimens is quite high, its lower limit is still higher than the lower limit of the control specimens' result and the design values according to AASHTO.

Another set of coupon specimens was tested after it was conditioned in a deicing solution at room temperature. A visual inspection did not reveal any change in the specimen's surface. The average weight of the conditioned facesheet and the web layer coupon specimens was increased by approximately 0.50% and 0.40%, respectively, due to solution absorption (also known as plasticization). The average results of the facesheet coupons showed that the tensile strength and tensile modulus of elasticity (Figs. 11 and 12) were 31.6 ksi (217.9 MPa) and 1949.6 ksi (13.4 GPa), respectively. The average results of the ultimate tensile strength and tensile modulus of elasticity of the web core coupons were 21.5 ksi (148.2 MPa) and 1360.7 ksi (9.4 GPa), respectively (Figs. 13 and 14). The residual tensile strength, when compared with the facesheet coupon results, was approximately 85.2%, while the residual tensile modulus was approximately 96%. The residual tensile strength and residual tensile modulus of elasticity of the web core coupons were approximately 83.3% and 80.5%, respectively.

A series of coupon specimens was also conditioned in a deicing solution at an elevated temperature of 122°F (50 °C). The specimens were then tested under tension. This regimen did not affect the specimens' appearance when compared to the control specimens. The average weight of the conditioned facesheet and web layer coupon specimens was increased by approximately 1.21% and 0.99%, respectively, due to solution absorption. It should be noted here that the elevated temperature helped accelerate absorption. The results for the web core coupons were missed during the test due to a problem that occurred in the data acquisition. The average results taken from the facesheet coupons revealed that the tensile strength was 31.3 ksi (215.8 MPa), and the tensile modulus of elasticity was 1738.6 ksi (11.9 GPa), as shown in Figs. 11 and 12, respectively. A comparison of the results with the control coupon specimens showed that the residual tensile strength was approximately 84.4%, while the residual tensile modulus was approximately 85.6%.

Finally, a set of coupons was conditioned under a series of freeze–thaw, mid–high temperatures, and mid–high relative humidity cycles in a computer-controlled environmental chamber for 350 cycles (1752 h). Unfortunately, the results for the web core coupons were lost during the test. The average results for the facesheet coupons indicated a tensile strength of 34.9 ksi (240.6 MPa) and a tensile modulus of elasticity of 2040 ksi (14.0 GPa) (see Figs. 11 and 12). Comparing the results with the control coupon specimens showed that the residual tensile strength was approximately 94%, while the residual tensile modulus was approximately 100.5%.

3.2. Four-point bending flexural testing results

The PU sandwich panels were removed and thoroughly inspected for signs of damage after they had been in the chamber for the required number of days. A visual inspection revealed that the outer surface had lost some of its brightness. The sectional dimensions of each conditioned panel did not change when compared to their original dimensions. The weight, however, did increase by approximately 0.5%. The PU panels were then instrumented with strain gauges and placed into the static loading test setup (Figs. 9 and 10). The applied load versus the mid-span deflection of both the conditioned and the control PU sandwich panels is illustrated in Fig. 17. All of the panels exhibited nearly the same tendency: they behaved almost linearly up to failure. The control and conditioned PU panels failed at an average load of approximately 17.8 kips (79.2 kN) and 13.5 kips (60.1 kN) at a mid-span deflection of approximately 1.01 in. (25.65 mm) and 0.69 in. (17.53 mm), respectively. Accordingly, the average ultimate load of the environmentally conditioned PU panels indicated a noticeable decrease in static flexural strength by approximately 24% compared to the control PU panels. In addition, the average stiffness exhibited by both of the conditioned PU panels was approximately 11% higher than that exhibited by the control PU panels. These results are summarized in Table 6.

Failure of the two control panels occurred by two failure phases: an initial failure mode that occurred by the outward skin wrinkling on the top facesheet (see Fig. 18a) followed by an ultimate failure mode that occurred due to excessive compressive stresses in the top facesheet under the loading points, as depicted in Fig. 18b. The conditioned PU

Table 4
Summary of web core coupons' tensile strength results.

Tensile strength	Control	Ultraviolet effect	Deicing effect
Mean, ksi (MPa)	25.8 (177.9)	27.4 (188.9)	21.5 (148.2)
SD, ksi (MPa)	0.17 (1.2)	0.61 (4.2)	0.74 (5.1)
C.V (%)	0.65	2.24	3.45

Table 5
Summary of web core coupons' modulus of elasticity results.

Modulus of elasticity	Control	Ultraviolet effect	Deicing effect
Mean, ksi (GPa)	1691 (11.7)	1839.8 (12.7)	1360.7 (9.4)
SD, ksi (GPa)	121.74 (0.84)	38.13 (0.26)	87.52 (0.60)
C.V (%)	7.20	2.07	6.43

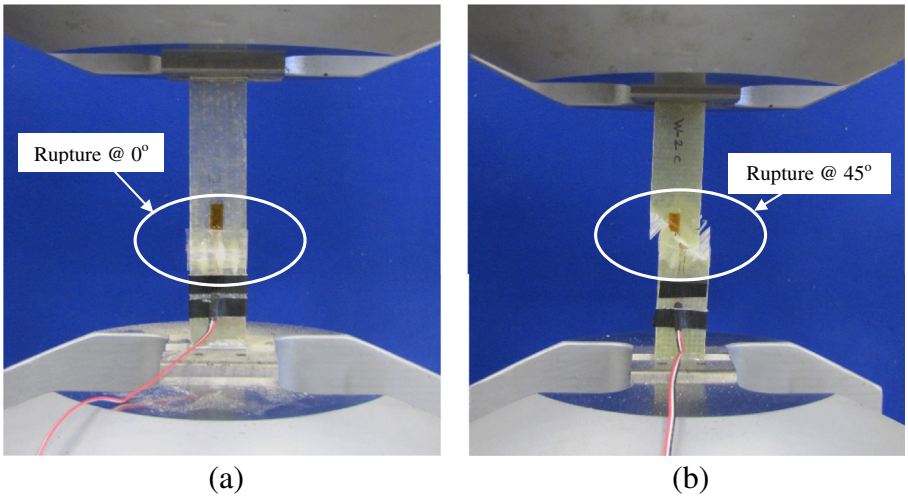

Fig. 15. Failure modes: (a) facesheet coupon and (b) web core coupon.

panels failed under excessive compressive stresses in the top facesheet under the loading points, as depicted in Fig. 19. Outward skin wrinkling did not occur, compared to the control panels, as the static flexural load that causes wrinkling was not reached due to the load reduction (see Fig. 20).

The strain gauges that were bonded to the bottom and top faces at the mid-span of the panels were measured to test the curve's linearity. The load versus strain curves for both the control and the conditioned PU sandwich panels are illustrated in Fig. 20. The average maximum tensile strain recorded (bottom facesheet) for the control PU panels was 0.00907 in./in. (mm/mm) at an average load of approximately 17.8 kips (79.2 kN). For the environmentally conditioned PU panels, it was approximately 0.006782 in./in. (mm/mm). Thus, the strain was reduced by nearly 25%. The wrinkling phenomena that occurred in the control PU panels can be observed in the response of the top strain gauge's curve (see Fig. 20). The reading exhibited both nonlinearity and a reversal of direction before it reached the ultimate load. The top strain gauge readings in the environmentally conditioned PU panels had a linear response up to failure, confirming the previous observation that outward skin wrinkling did not occur.

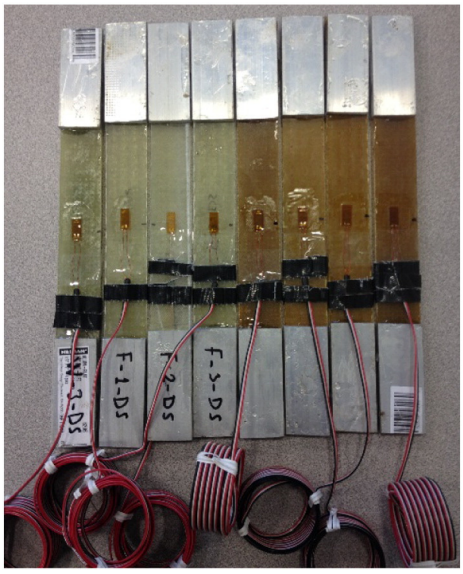

Fig. 16. Color comparision between the control (left) and UV conditioned (right) specimens.

4. Discussion and summary of results

4.1. GFRP laminates

The ultraviolet radiation increased both the ultimate tensile strength and the tensile modulus of elasticity for both the facesheet and the web core coupons by approximately 3% and 10%, respectively. This increase is assumed to be due to the post-curing of the resin when exposed to elevated temperatures. For example, exposure to an elevated temperature can facilitate the linking of these polymers, causing additional curing. Manufactured civil composites are seldom fully cured. Thus, thermal exposure does not always harm the FRP composites as long as the temperature is below the Tg of the matrix. This finding agrees with the results conveyed by Connolly et al. [20]. In addition, as part of the product development process for the polyurethane resin, the manufacturer conducted its own UV testing on coupon specimens. The results showed that the degradations in strength and stiffness were less than 2%, which reasonably confirms this study's, taking into account the scatter on results.

The deicing solution, under a room temperature and under an elevated temperature, adversely affected the ultimate tensile strength and tensile modulus of elasticity of both the facesheet and the web core coupons. These reductions agree with the results reported by Jamond et al. [18] and Malvar et al. [19]. The average degradation was

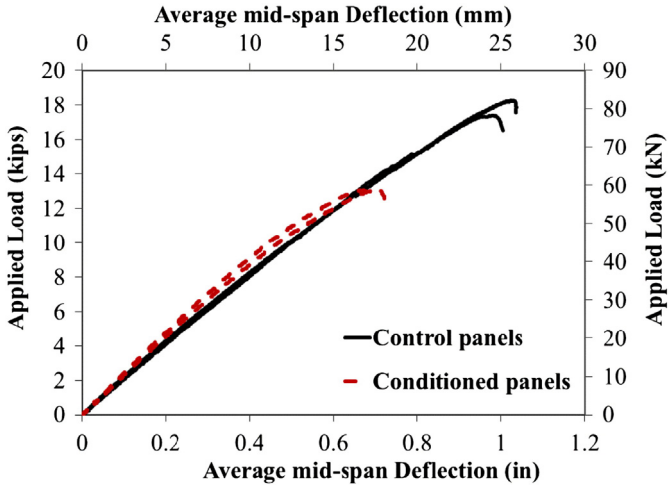

Fig. 17. Applied load vs. mid-span deflection.

Table 6
Structural behaviors of four-point bending flexural results.

Condition	Control Panels			Conditioned Panels		
	Ultimate load capacity, kips (kN)	Flexural stiffness, kip.in^2 (kN.m^2)	Failure mode	Ultimate load capacity, kips (kN)	Flexural stiffness, kip·in^2 (kN·m^2)	Failure mode
Mean	17.8 (79.2)	26,221.35 (7525)	Wrinkling + compressive failure	13.5 (60.0)	29,105.70 (8353)	Compressive failure
SD	0.43 (1.91)	748.65 (214.8)		0.10 (0.44)	870.00 (249.6)	
CV (%)	2.41	2.86		0.74	2.98	

approximately 16% in the tensile strength and 12% in the tensile modulus of elasticity for both the facesheet and web core coupons. This reduction can be attributed to the high percentage of voids, which can easily be seen by the naked eye. These voids increased the permeability and subsequent diffusion of light atomic weight free salt ions into the GFRP composite, causing differential swelling stresses and degradation to the physical properties of the fiber. This result suggests that quality control during the manufacturing process not only controls the strength of the composites, but also affects their resistance to environmental effects. Moisture has also been shown to act as a plasticizer in cured thermosets by causing the polymer to swell. This swelling can lead to increased internal stresses and micro-cracking in the composite. Moisture may also have deleterious effects to the matrix-fiber interface. Reduction under an elevated temperature, in the deicing solution, was close to the aging regimen at room temperature (within the normal scatter). Although the purpose of using a higher temperature was to accelerate absorption, the high temperature seemed to post-cure the polymer, which downplayed the effect of the deicing solution on the exposed coupons.

The thermal cycling conditioning reduced the ultimate tensile strength and increased the tensile modulus of elasticity for the facesheet coupon specimens by approximately 6% and 0.5%, respectively. This increase was likely a result of post-curing of the resin during the high temperature cycles. The strength reduction could be related to the freeze–thaw cycles. Due to the mismatch of the coefficient of thermal expansion (CTE), microcracks and voids in the polymer matrix occurred and caused progressive damage within the fiber materials due to the expansion and contraction cycles (thermal fatigue) of the entrapped water. These causes were similar to those described by Karbhari and Pope [14], GangaRao et al. [15], and Verghese et al. [17].

4.2. PU sandwich panels

The stiffness of the thermal cycling conditioned PU sandwich panels was increased by between 8% and 14%. This increase is likely due to the extended curing of the polyurethane resin during high temperature sequences. It was assumed that the elevated temperatures could enhance the curing of the resin because it is common that the GFRP composites are not fully cured (due to insufficient time). Thus, exposure to elevated temperatures that is higher than the curing temperature can facilitate the linking of these polymers, causing additional curing. This additional curing will increase the stiffness of the GFRP material.

In contrast, the thermal cycling (freeze–thaw) conditioning regimen negatively affected the material property of the fibers in terms of their flexural strength. This loss of strength (24%) could be related to the freeze–thaw cycles. Due to the mismatch of the coefficient of thermal expansion (the polymeric resin coefficient is generally an order of magnitude higher than that of the fiber), microcraks and voids in the polymer matrix and in the matrix-fiber interface occurred, causing progressive damage within the fiber materials due to the expansion and contraction cycles (thermal fatigue) of the entrapped water. This reduction is consistent with the FHWA guidelines on composite deck designs. These guidelines recommend an environmental durability factor of 0.65 to account for the degradation of properties over time and represent a 35% decrease in strength.

It should be noted that the same trends exhibited in testing the conditioned GFRP coupon specimens are similar to the results of the mid-scale panels, where the strengths of the test specimens decreased and stiffness increased. It is expected that web core coupons would yield similar results, bringing the total reduction to 24%. Yet again, the design of FRP bridge deck panels is often controlled by stiffness rather than strength. Therefore, such structures tend to be designed as small as 10–15% of their ultimate strength [31].

5. Conclusion

GFRP laminates and PU sandwich panels were successfully manufactured using a VARTM process in which a new polyurethane resin was used as a matrix. These specimens were conditioned under different conditioning regimens. Tensile strength tests and four-point loading tests were then performed on the GFRP laminates and the PU sandwich panels, respectively. The degradation was determined in terms of ultimate strength and stiffness. The following conclusions were drawn from this study:

i. The PU sandwich panels displayed linear-elastic behavior throughout the majority of their response during the static flexural testing with only a slight decrease in stiffness near failure.

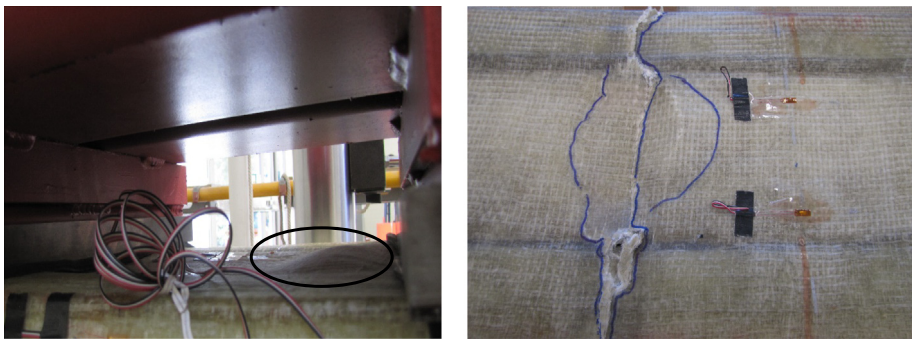

Fig. 18. Failure modes: (a) initial failure due to outward compression facing wrinkling, and (b) ultimate failure due to compression failure of the facesheet under loading points.

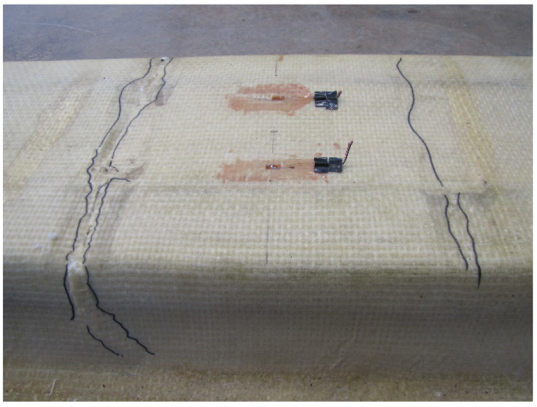

Fig. 19. Compressive failure of the facesheet under loading points.

ii. Neither the tensile strength nor the tensile modulus was adversely affected when the facesheet and web core coupons were exposed to ultraviolet radiation. Instead, each increased as a result of the post-curing of the resin system.
iii. The deicing solution, under both room temperature and elevated temperature, reduced the ultimate tensile strength and the tensile modulus of elasticity in both the facesheet and the web core coupons.
iv. Thermal cycling conditioning reduced the ultimate tensile strength and increased the tensile modulus of elasticity for the facesheet coupon specimens by approximately 6% and 0.5%, respectively.
v. The flexural behavior of the PU sandwich panels exposed to thermal cycling in an environmental chamber resulted in a 24% degradation in the ultimate strength but a slight increase in stiffness. Failure of the conditioned panels under the subsequent static loading occurred in the same manner as the control panels.
vi. Manufacturing these specimens utilizing polyurethane resin within the VARTM process resulted in a strength reduction that is consistent with FHWA guidelines. The FHWA recommends an environmental durability factor of 0.65 to account for properties degrading over time and represents a 35% decrease in strength.

As with most FRP deck panels, stiffness is always controlled their design. This study showed that the only degradation that occurred in the tensile modulus of elasticity of the GFRP coupons was due to the effects of the deicing solution. This reduction was mainly attributed to the high percentage of voids. It is believed that this reduction would be overcome or reduced if the quality control during the manufacturing process were improved. Therefore, the formation of highly cross-linked and excellent thermal stability of the new-generation two-part thermoset polyurethane enhanced the durability performance of the proposed PU sandwich deck panels. Generally, the expected in-service stress levels in the PU panel maintain the potential for long-term durability.

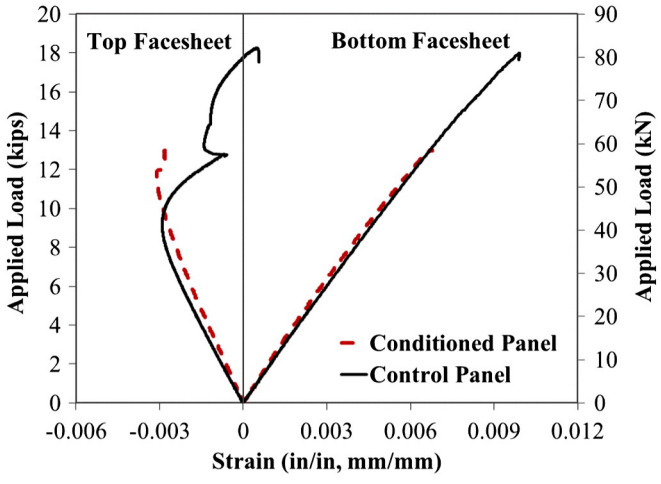

Fig. 20. Applied load vs. mid-span strain.

Acknowledgments

The authors acknowledge the Missouri Department of Transportation (MoDOT) (TRyy1203) and the National University Transportation Center (NUTC) (DTRT06-G-0014) at Missouri University of Science and Technology for sponsoring this research study.

References

[1] Kirk RS, Mallett WJ. Highway bridge conditions: issues for Congress. Congressional Research Service, Report to congress. Contract No. R43103; 2013.
[2] Ellis Z. "Corrosion cost and preventive strategies in the United States", FHWA-RD-01-156; 2011.
[3] Karbhari VM. Durability of composites for civil structural applications. Cambridge England: Woodhead Publishing Limited; 2007.
[4] Robert M, Wang P, Cousin P, Benmokrane B. Temperature as an accelerating factor for long-term durability testing of FRPs: should there be any limitations? J Compos Constr 2010;14(4):361–7.
[5] Sousa J, Correia J, Cabral-Fonseca S, Diogo A. Effects of thermal cycles on the mechanical response of pultruded GFRP profiles used in civil engineering applications. Compos Struct 2014:720–31. http://dx.doi.org/10.1016/j.compstruct.2014.06.008.
[6] Wu H, Yan A. Durability simulation of FRP bridge decks subject to weathering. Compos Part B: Eng 2013:162–8. http://dx.doi.org/10.1016/j.compositesb.2013.03.018.
[7] Li H, Xian G, Lin Q, Zhang H. Freeze–thaw resistance of unidirectional-fiber-reinforced epoxy composites. J Appl Polym Sci 2012:3781–8. http://dx.doi.org/10.1002/app.34870.
[8] Shen CH, Springer GS. Effects of moisture and temperature on the tensile strength of composite materials. In: Springer GS, editor. Environmental Effects on Composite Materials. Technomic Publication Co.; 1981. p. 79.
[9] Giori C, Yamauchi T. Effects of ultraviolet and electron radiations on graphite-reinforced polysulfone and epoxy resins. J Appl Polym Sci 1984;29:237.
[10] Azwa ZN, Yousif BF, Manalo AC, Karunasena W. A review on the degradability of polymeric composites based on natural fibres. Mater Des 2013;47:424–42.
[11] Korach CS, Chiang FP. Characterization of carbon fiber-vinylester composites exposed to combined UV radiation and salt spray. ECCM15—15th European conference on composite materials; 2012 [Venice, Italy].
[12] Caceres A, et al. Salt-fog accelerated testing of glass fiber reinforced polymer composites. DTIC Document; 2002.
[13] Hollaway LC. A review of the present and future utilisation of FRP composites in the civil infrastructure with reference to their important in-service properties. Construct Build Mater 2010;24(12):2419–45.
[14] Karbhari VM, Pope G. Effect of cold region type environment on impact and flexure properties of glass/vinyelester composites. ASCE J Cold Reg Eng 1993;**8**(**1**):1–20.
[15] GangaRao HVS, Vijay PV, Dutta PK. Durability of composites in infrastructure. Proceedings of Corrosion, 1995. Paper No. 550; 1995. p. 1–8.
[16] Lapoez-Anido R, Michael AP, Sandford TC. Freeze–thaw resistance of fiber-reinforced polymer composites adhesive bonds with underwater curing epoxy. J Mater civ eng 2004.
[17] Verghese NE, Hayes M, Garcia K, Carrier C, Wood J, Lesko JJ. Effects of temperature sequencing during hygrothermal aging of polymers and polymer matrix composites: the reverse thermal effect. Fiber Composites in Infrastructure, Proceedings of the Second International Conference on Fiber Composites in Infrastructure ICCI '98, 2. ; 1998. p. 720–39.
[18] Jamond RM, Hoffard TA, Novinson T, Malvar LJ. Composites in simulated marine environments. NFESC Special Publication SP-2083-SHR; 2000.
[19] Malvar LJ, Jamond RM, Hoffard TA, Novinson T. GFRP composites in simulated marine environments. 2nd international conference on durability of FRP composites for construction, CDCC'02, Montreal, Quebec, Canada; 2002. p. 191–202.
[20] Connolly M, King J, Shidaker T, Duncan A. Processing and characterization of pultruded polyurethane composites. Huntsman Enriching lives through innovation; 2006.
[21] Karakuzu R, Erbil E, Aktas M. Impact characterization of glass/epoxy composite plates: an experimental and numerical study. Compos Part-B 2010;41:388–95.
[22] Bareis D, Heberer D, Connolly M. Advances in urethane composites resins with tunable reaction times. Huntsman Polyurethanes Auburn Hills, MI: American Composites Manufacturers Association Ft. Lauderdale, Florida; 2011 1–7.
[23] Tuwair H, Hopkins M, Volz J, ElGawady M, Mohamed M, Chandrashekhara K, Birman V. Evaluation of sandwich panels with various polyurethane foam—cores and ribs. Compos Part B 2015;79:262–76.
[24] American Society of Testing and Materials. ASTM Standard Test Method for Tensile Properties of Polymer Matrix Composite Materials (ASTM D3039/D3039M-08). West Conshohocken, Pennsylvania: ASTM International; 2008.

[25] American Society of Testing and Materials. ASTM standard practice for exposing nonmetallic materials in accelerated test devices that use laboratory light sources (G151-10). West Conshohocken, Pennsylvania: ASTM International; 2010.
[26] American Society of Testing and Materials. ASTM standard test method for standard practice for operating fluorescent light apparatus for UV exposure of nonmetallic materials (G154-00a). West Conshohocken, Pennsylvania: ASTM International; 2000.
[27] American Society of Testing and Materials. ASTM standard test method for standard practice for fluorescent ultraviolet (UV) exposure of photodegradable plastics (D2508-14). West Conshohocken, Pennsylvania: ASTM International; 2014.
[28] American Society of Testing and Materials. ASTM standard test method for resitance of concrete to rapid freezing and thawing (C666/C666M-08). West Conshohocken, Pennsylvania: ASTM International; 2008.
[29] Micelli F, Myers J. Durability of FRP-confined concrete. Proc inst Civ Eng 2008; 161(4):173–85.
[30] American Society of Testing and Materials. ASTM standard test method for flexural properties of sandwich constructions (C393/C393M-11e1). West Conshohocken, Pennsylvania: ASTM International; 2011.
[31] Tuwair H, Volz J, ElGawady M, Mohamed M, Chandrashekhara K, Birman V. Testing and evaluation of polyurethane−based GFRP sandwich bridge deck panels with polyurethane foam core. J Bridg Eng 2015 http://dx.doi.org/10.1061/(ASCE)BE.1943-5592.0000773, 04015033.